



HAL
open science

A multi-sensor approach to monitor the ongoing restoration of edaphic conditions for salt marsh species facing sea level rise: An adaptive management case study in Camargue, France

Aurélie Davranche, Céline Arzel, Pierre Pouzet, A. Rita Carrasco, Gaëtan Lefebvre, Dimitri Lague, Marc Thibault, Alice Newton, Cyril Fleurant, Mohamed Maanan, et al.

► To cite this version:

Aurélie Davranche, Céline Arzel, Pierre Pouzet, A. Rita Carrasco, Gaëtan Lefebvre, et al.. A multi-sensor approach to monitor the ongoing restoration of edaphic conditions for salt marsh species facing sea level rise: An adaptive management case study in Camargue, France. *Science of the Total Environment*, In press, pp.168289. 10.1016/j.scitotenv.2023.168289 . hal-04281757v1

HAL Id: hal-04281757

<https://hal.science/hal-04281757v1>

Submitted on 8 Nov 2023 (v1), last revised 13 Nov 2023 (v2)

HAL is a multi-disciplinary open access archive for the deposit and dissemination of scientific research documents, whether they are published or not. The documents may come from teaching and research institutions in France or abroad, or from public or private research centers.

L'archive ouverte pluridisciplinaire **HAL**, est destinée au dépôt et à la diffusion de documents scientifiques de niveau recherche, publiés ou non, émanant des établissements d'enseignement et de recherche français ou étrangers, des laboratoires publics ou privés.



Distributed under a Creative Commons Attribution 4.0 International License

Journal Pre-proof

A multi-sensor approach to monitor the ongoing restoration of edaphic conditions for salt marsh species facing sea level rise: An adaptive management case study in Camargue, France

Aurélie Davranche, Céline Arzel, Pierre Pouzet, A. Rita Carrasco, Gaëtan Lefebvre, Dimitri Lague, Marc Thibault, Alice Newton, Cyril Fleurant, Mohamed Maanan, Brigitte Poulin



PII: S0048-9697(23)06916-4

DOI: <https://doi.org/10.1016/j.scitotenv.2023.168289>

Reference: STOTEN 168289

To appear in: *Science of the Total Environment*

Received date: 27 March 2023

Revised date: 31 October 2023

Accepted date: 31 October 2023

Please cite this article as: A. Davranche, C. Arzel, P. Pouzet, et al., A multi-sensor approach to monitor the ongoing restoration of edaphic conditions for salt marsh species facing sea level rise: An adaptive management case study in Camargue, France, *Science of the Total Environment* (2023), <https://doi.org/10.1016/j.scitotenv.2023.168289>

This is a PDF file of an article that has undergone enhancements after acceptance, such as the addition of a cover page and metadata, and formatting for readability, but it is not yet the definitive version of record. This version will undergo additional copyediting, typesetting and review before it is published in its final form, but we are providing this version to give early visibility of the article. Please note that, during the production process, errors may be discovered which could affect the content, and all legal disclaimers that apply to the journal pertain.

Title:

A multi-sensor approach to monitor the ongoing restoration of edaphic conditions for salt marsh species facing sea level rise: an adaptive management case study in Camargue, France.

Authors :

Aurélie Davranche^{a*}, Céline Arzel^b, Pierre Pouzet^c, A. Rita Carrasco^d, Gaëtan Lefebvre^e, Dimitri Lague^f, Marc Thibault^e, Alice Newton^d, Cyril Fleurant^g, Mohamed Maanan^h, Brigitte Poulin^e

Corresponding author: *Aurélie Davranche, aurelie.davranche@helsinki.fi

Affiliations

a Lammi Biological Station, Department of Forest Sciences, University of Helsinki, Pääjärventie 320, 16900, Lammi, Finland and University of Angers, France.

b Department of Biology, FI-20014, University of Turku, Finland

c L@bisen, Institut Supérieur de l'Électronique et du Numérique (ISEN)

d Centre for Marine and Environmental Research (CIMA), University of Algarve, Campus of Gambelas, 8005-139 Faro, Portugal,

e Tour du Valat, Research Institute for the Conservation of Mediterranean Wetlands, Le Sambuc, 13200 Arles, France

f Univ Rennes, CNRS, Géosciences Rennes, UMR 6118, 35000 Rennes, France

g Univ Angers, Nantes Université, Le Mans Univ, CNRS, LPG, F-49000 Angers, France

h LETG UMR CNRS 6554, University of Nantes, CEDEX 3, 44312 Nantes, France

Abstract

The Camargue or Rhône delta is a coastal wetland in southern France of which parts formerly devoted to salt production are undergoing a renaturation process. This study assessed a multisensor approach to investigate the link between sediment size distribution, habitat development mapped with Worldview 2, flooding durations estimated with time series of SENTINEL 2 images and elevation modelled with a LIDAR point cloud in former saltworks. A Random Forest classification algorithm was used to map the vegetation distributions of *Sarcocornia fruticosa* and *Arthrocnemum macrostachyum*, main representatives of the NATURA 2000 "Mediterranean and thermo-Atlantic halophilous scrubs (*Sarcocornetea fruticosi*)" habitat on the site. The best habitat map was obtained when considering the species separately. The random forest Out-of-bag errors were 1.43% for *S. fruticosa* and 2.18% for *A. macrostachyum*. Both species were generally distributed on different elevation and flooding duration zones considering mean values. Flooding duration was estimated with the Water In Wetland index (WIW) based on 15 Sentinel-2 scenes. Two models related to sediment grain size distribution were developed: one predicting the flooding duration and one predicting the halophilous scrub distribution. Maps of flooding duration, sediment grain size distribution and elevation highlighted two main zones in the study area: a western section with coarser sediments, shorter flooding durations and higher elevations under sea influence; an eastern section with finer sediments, longer hydroperiods and lower elevations under a historic river influence. This multidisciplinary approach offers perspectives for using space-based data over large scales to monitor changes in edaphic conditions of coastal areas facing natural and anthropogenic forcings. The results call for further investigations to predict the dynamic distribution of other coastal habitats following climate change impacts, such as sea level rise.

Keywords

elevation, flooding duration, halophilous scrubs, nature-based solution, remote sensing, sediment distribution.

Figures captions

Fig. 1. Workflow of the approach

Fig. 2. Location and delimitation of the study area, the former saltworks of Salin de Giraud in Camargue (B), south of France (A). Labels refer to some hydrological units defined at the time of salt production.

Fig. 3. Location of the sediment sampling points in the former saltworks.

Fig. 4. Reflectance of *S. fruticosa* and *A. macrostachyum*, measured with a Jaz spectrometer in the field on 7-8 September 2016.

Fig. 5. Classification (spatial resolution 2 m) of perennial halophilous scrubs (*S. fruticosa* and *A. macrostachyum*) placed on (A) the interpolation of median grain size (D50mm; discretization based on quantile, spatial resolution 10 m), (B) the DTM (spatial resolution 50 cm, discretization based on quantiles) and (C) the flooding duration from 0 (always dry) to 15 (always flooded) (spatial resolution = 10) in the former saltworks of Salin de Giraud. (D) is a 3D animation starting from North-West and finishing South-East, based on a set of camera positions placed on the combination of the 3 maps; the median grain size was extracted for each pixel of halophilous scrubs placed on the flooding duration map shaped with the DTM in three dimensions (vertical scale = 4, tile resolution = 200 px, skirt height = 1, offset = 1).

Fig. 6: Comparison of mean elevation of both species on both sides of the dyke (*S.fruticosa*_N = *S. fruticosa* at northeast from the dyke, *S.fruticosa*_S = *S. fruticosa* southwest of the dyke; *A.macrostachyum*_N = *A. macrostachyum* from northeast of the dyke, *A.macrostachyum*_S = *A. macrostachyum* from southwest of the dyke), bars representing the range of elevation values from minimum to maximum where species can be found according to the random forest classification. The different letters (a, b, c, d) identify mean values that are significantly different.

Fig. 7. Comparison of mean flooding duration of both species on both sides of the dyke (*S.fruticosa*_N = *S. fruticosa* at northeast from the dyke, *S.fruticosa*_S = *S. fruticosa* southwest from the dyke; *A.macrostachyum*_N = *A. macrostachyum* from northeast of the dyke, *A.macrostachyum*_S = *A. macrostachyum* from southwest of the dyke), bars representing the range of flooding duration from minimum to maximum where species can be found according to the random forest classification. The different letters (a, b, c, d) identify mean values that are significantly different.

Fig. 8. Flooding duration (duration from 0 to 15 dates) grouped and ranked according to the pairwise analysis with *Kruskall-Wallis* test and bonferroni p adjustment of their mean values of elevation on the DTM. Letters

a to h refers to group identifiers (different group = significant difference), and bars are range values (min-max).

1. Introduction

The state and evolutionary trends of coastal wetland systems are the result of complex interactions between hydrodynamic, ecological, hydrological and sediment transport processes, forced by tidal fluctuations (Fagherazzi et al., 2020). Eco-geomorphological processes are paramount for their evolution, with straightforward feedbacks between drivers and vegetation development (Belluco et al., 2006; van Proosdij et al., 2006). Salt marsh vegetation increases the stability of the soil through its roots and dissipates the flow through stems and leaves, promoting the accretion of the marsh (Silvestri et al., 2003). Hence, vegetation changes can initiate morphological changes, while geomorphological changes can impact salt marsh plants. In the Mediterranean region, the habitat NATURA 2000 "Mediterranean and thermo-Atlantic halophilous scrubs (*Sarcocornetea fruticosi*)" conservation status is "Unfavourable bad" (Habitats Directive 92/43/EEC). In Camargue (southern France), one of the most important regions for its conservation, its coverage decreased with the development of the saltworks industry from 1856 and agriculture. The Camargue is one of the largest and most biodiverse Mediterranean wetlands (Fraixedas et al., 2019). It was designated as a Ramsar site in 1986 for its international importance for nesting, staging and wintering waterbirds (Mathevet et al., 2015). About 70% of the Camargue lies within 1 m above mean sea level. Hence, it is extremely vulnerable to flooding. In the 1860s, dykes were built to prevent flooding of its southern coastal part. The consequence was a polderization of the delta with a reduction in sediment inflow from the Rhône River that affected dune formation and increased coastal erosion. These changes have been accelerated by sea-level rise due to climate change (Parc naturel régional de Camargue et al., 2022). In this Mediterranean region, the annual maximum observed sea-level height, since 1961, increases by 4 mm/year associated with a frequency and a speed of wind blowing from 100° to 120° sectors, that tends to push the water toward the coast. Coastal erosion progressively reduced the beach width and made hydrodynamics phenomena more intense (Ullmann et al., 2007).

Since 2010, the Conservatoire du Littoral, a public organization that protects coastal areas in France, has progressively purchased 65 km² of former saltworks near Salin-de-Giraud. It was exploited for industrial salt production with major transformations between the 1950's and early 1970's. The site hosts large areas of

lagoons, Mediterranean salt steppes, coastal dunes and wooded dunes. This area is under the protection of Conservatoire du littoral since 2010 and presents the greatest diversity of natural habitats in Camargue (Conservatoire du Littoral, 2015). It is part of the Natura 2000 network and includes 22 habitats targeted by the European Habitat Directive. It hosts 541 plant species (including 30 protected species) and 302 bird species and is an important staging area for waterbirds. The Conservatoire du littoral (2015) is promoting an ecosystem-based management process of these former saltworks, following a well-defined adaptive management plan. One of the main objectives of this management strategy is to increase resilience to sea level rise and coastal erosion. The restoration of natural flooding patterns has favoured the development of halophilous vegetation (Conservatoire du Littoral, 2015), which improves salt marsh ecological functioning and stability, since the loss of this vegetation is likely to exacerbate the effects of sea level rise on coastal marshes (Ivajnsiĉ et al., 2018).

The severity and magnitude of natural and human pressures being exerted on wetland ecosystems such as the Camargue, (Newton et al., 2020), justify the implementation of restoration approaches with adaptive management. The former saltworks of Camargue offer a unique case study and a rare example of applied adaptive management in France, despite scientists calling for this process to be included in the planning of protected areas (Bioret et al., 2008).

Adaptive management is an iterative process relying on the co-design of the management of natural systems with stakeholders, by developing interdisciplinary approaches, using scientific knowledge to define management targets, through the development of environmental assessment plans, and the implementation of a control fluxes to assess the results of the implementation and evaluate the success of the restoration process (Bobbink et al., 2006; Olsson et al., 2004). In this process, feedbacks complete the cycle of planning, implementation, and evaluation (Lyons et al., 2008). Monitoring is thus a crucial component of an informed process for supporting management decisions in restored ecosystems. Designing a monitoring plan should start from the decision context and provide knowledge on uncertainties (Lyons et al., 2008). Since remote sensing is an effective ecological survey tool that can be easily updated (Zedler and Kercher, 2005), it can play an important role in the monitoring of adaptive management of habitats (El Mahrad et al., 2020). Satellite remote sensing is one of the most suitable methods for this purpose (Blount et al., 2022; Campbell and Wang, 2019; Hu et al., 2021), as it allows comprehensive and long-term observations over broad areas,

enabling the characterization of land surface changes in a wide variety of spatial and temporal scales. Hence, it can provide simultaneous and repetitive coverage over large areas, allowing fast, frequent and consistent monitoring (Blount et al., 2022). Over the past decade, several remote sensing tools have been developed with input from managers to monitor the vegetation distribution in the Camargue wetlands (Davranche et al., 2010), ecological state of its reed marshes (Poulin et al., 2010) and flooding duration (Davranche et al., 2013; Lefebvre et al., 2019).

The former saltworks of Salin de Giraud have evolved rapidly in terms of water pathway change, salt marsh vegetation development and dune dynamic (Parc naturel régional de Camargue et al., 2022). The adaptive management approach of the Conservatoire du littoral is an invaluable resource of knowledge likely to be applied to other coastal areas facing similar natural and human threats. However, the monitoring phase of this adaptive management process imposes significant costs with a paradoxical configuration for the managers as field data collection takes significant time (*i.e.*, several years) to cover the entire study area, while the site experiences rapid intra-annual changes. In this context, this study assesses the potential of using remote sensing and sediment analyses to monitor the dynamic of the former saltworks as part of the adaptive management plan implemented in these Mediterranean coastal lagoons in Camargue. We tested methods that combined (i) sediment size distribution analyses linked to vegetation changes and water inflows, and (ii) remote sensing analysis to obtain a synoptic view of vegetation development, flooding duration and elevation. The potential of multisource remote sensing data is discussed with regards to understanding vegetation dynamics, dune formation and hydrodynamics, in a context of sea level rise and land use change.

2. Methods

Our approach (Fig. 1) investigated the link between sediment size distribution collected in the field, halophilous scrub distribution mapped with Worldview 2, flooding durations calculated via time series of SENTINEL 2 images and elevation modelled with a LIDAR point cloud, to monitor the adaptive management applying nature-based solutions to restore anthropized lagoons.

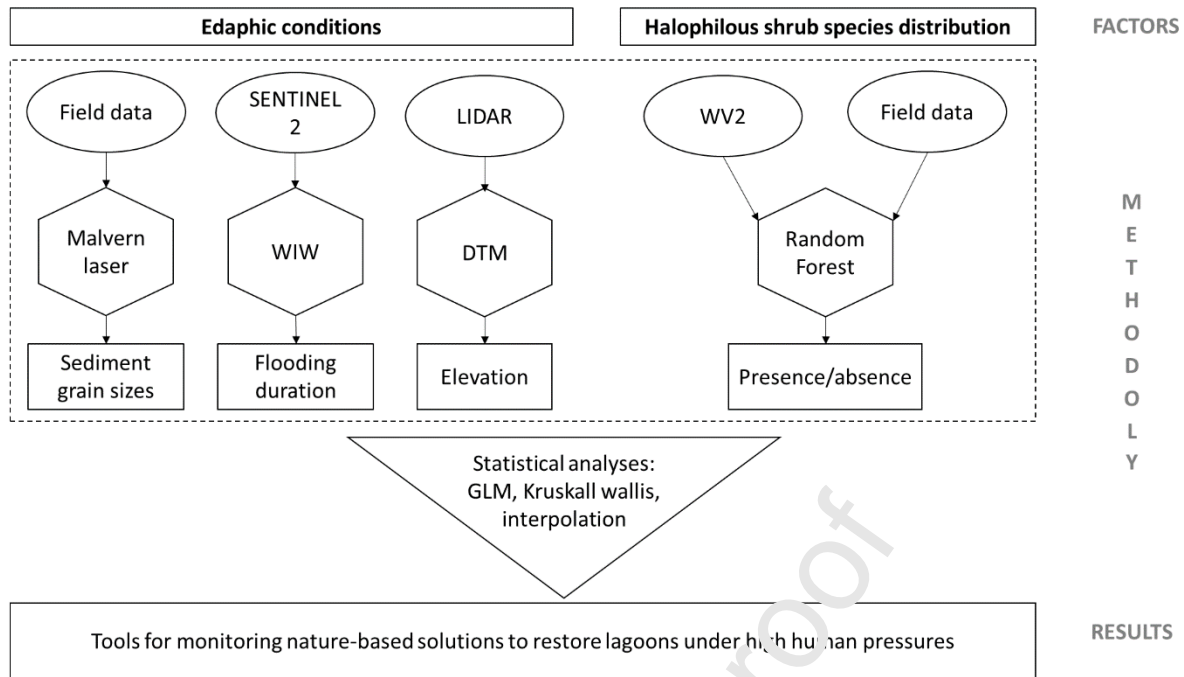


Fig. 1. Workflow of the approach.

2.1 Location and geomorphic dynamic of the study area

The Camargue is located in the eastern façade of the French Mediterranean arc (Fig 2A). From April to September, the sum of the evaporation exceeds precipitation, whereas after September rainfall outweighs the evaporation. Mean annual values of rainfall and water evaporation are respectively 600 mm and 1400 mm (Aubert et al., 2023). The Camargue coast has a microtidal range of about 30 cm (Rey et al., 2009). The dominant wind directions are NW, N and NE, which drive coastal currents to the west or east. Frequent strong winds lead to a homogenization of salt concentrations within the lagoons and force water exchanges between them (Höhener et al., 2010). Wind-controlled coastal currents transport significant amount of sand, which contribute to broadening the strand plain and coastal dunes along the Rhône shoreline (Rey et al., 2009). Our study area, the former saltworks of Salin de Giraud (Fig. 2C), is highly dynamic (Conservatoire du Littoral, 2015). Since 2010, the management strategy of the site focused on a progressive re-naturalization to restore the natural hydroperiods of the lagoons that were artificially flooded by seawater pumping at the time of salt production (Parc naturel régional de Camargue et al., 2022). To the north of the protective dyke, the water circulates by gravity, mainly from north to south, without a gravity outlet from Fangassier 1 (Fig. 2C), the latter's water level being essentially regulated by evaporation. To the south of the backward dyke, the waters flow by gravity in both directions, mainly depending on the water levels in the former salt parcels,

the prevailing winds and the sea level. Also, breaching of the former seafront dyke (Fig. 2C) has facilitated sea inflows in the southern part (Conservatoire du Littoral, 2015).

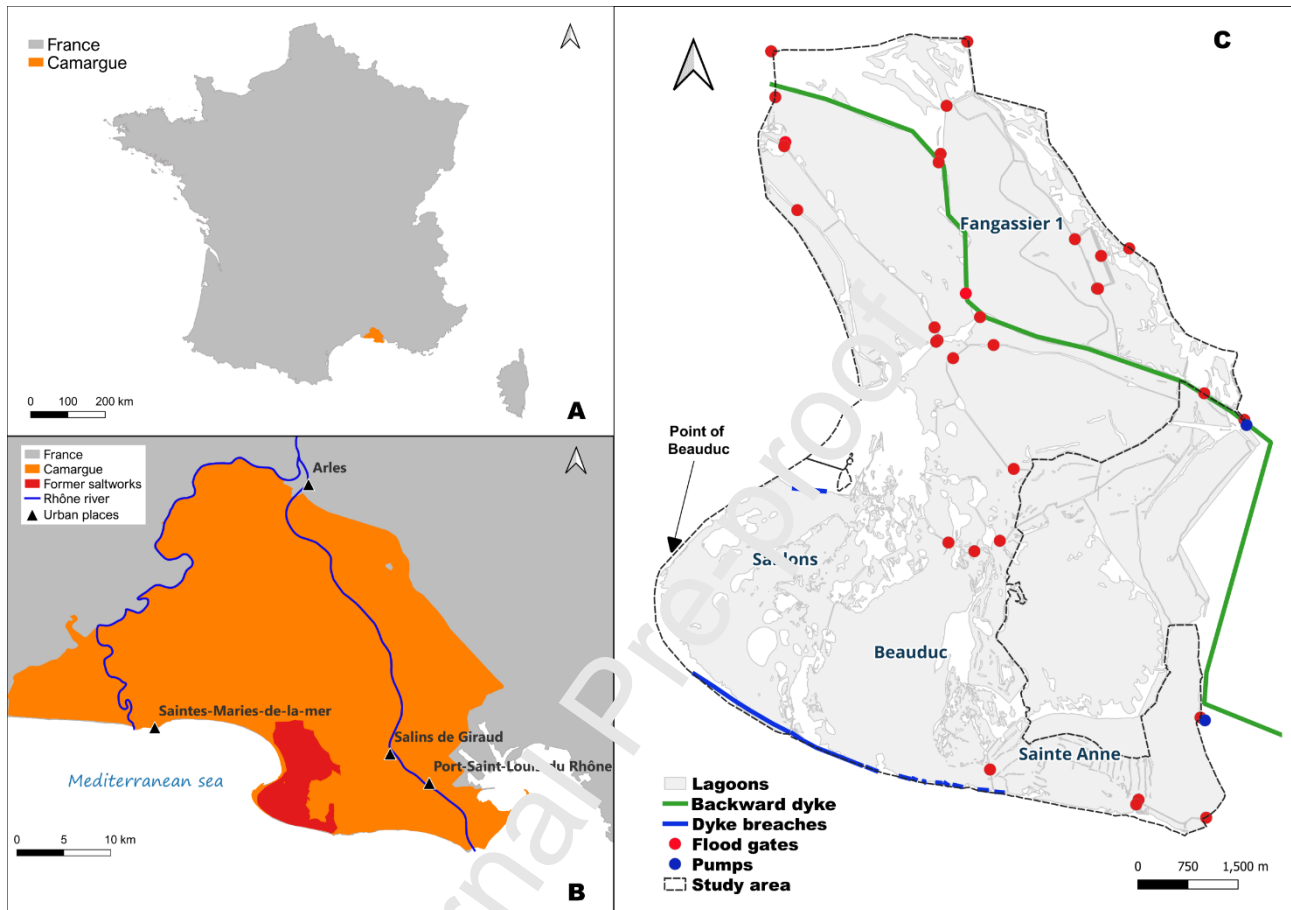


Fig. 2. Location and delimitation of the study area, the former saltworks of Salin de Giraud in Camargue (B), south of France (A). Labels refer to hydrological units defined at the time of salt production.

2.2 Studied species: ecological and edaphic conditions of development

This study focused on two species of halophilous scrubs i.e. *Arthrocnemum macrostachyum* and *Sarcocornia fruticosa*. They are the dominant species in the study area and form part of the habitat Natura 2000 coded 1420: Mediterranean and thermos-Atlantic halophilous scrubs (MHS), composed of flagship species such as *Arthrocnemum macrostachyum*, *Sarcocornia fruticosa*, *Sarcocornia fruticosa var. deflexa* and *Suaeda vera*. Its status is “Unfavourable-Bad (U2)” in the Mediterranean area (Evans and Arvela, 2011). MHS responds quickly to changes in hydrological regimes, which are well-known to impact its spatial distribution (Evans

and Arvela, 2011). Both study species are halophilic and perennial, being typically adapted to high soil anoxia and long flood duration by rainfall (Colmer and Flowers, 2008). *S. fruticosa* can tolerate salinity between 10 mM and 1000 mM of NaCl, with an optimal growth at 510 mM in warm saline habitats (Abdulrahman and Williams, 1981). Under prolonged salinity exposure, it accelerates its germination (Redondo-Gomez et al., 2007). The abundance of *S. fruticosa* can be increased through the provision of optimal salinity and silt-clay soil conditions (Landi and Angiolini, 2013). *A. macrostachyum* can tolerate higher salt and seasonal moisture variations than *S. fruticosa* (Rogel et al., 2000), although *S. fruticosa* can withstand high concentrations of salt year-round but it is not adapted to pronounced seasonal changes. In the Venice lagoon, *A. macrostachyum* usually develops at higher topographic levels than *S. fruticosa* (Silvestri et al., 2003). In the French Mediterranean area, *A. macrostachyum* is found on coarse sediment habitats characterised by higher salinity (Baumberger et al., 2012).

2.3 Vegetation data collection

From 2010 to 2013, Tour du Valat Research Institute (TDV) had inventoried 8% of the surface of the site following the Natura 2000 nomenclature to delimit habitats with polygons on a vector layer (1/10000 scale) using field knowledge and photointerpretation of aerial photographs acquired on 04/05/2011 by the French National Institute of Geographic and Forest Information. While Natura 2000 habitat typology provides valuable background information, it is not accurate enough for satellite-based mapping (Vanden Borre et al., 2011). Hence, in 2016 we performed a field campaign adapted to remote sensing analysis. We identified homogenous stands of halophilous scrubs and other land cover types distributed over the entire study area. Two hard-to-reach zones were surveyed with a drone (Phantom 4 - DJI) equipped with a visible camera (CMOS 1") to locate homogeneous stands of vegetation on newly formed dunes. The sample totalled 2 011 points (Table A.1) with 76 points of *A. macrostachyum* and 84 points of *S. fruticosa*. For each sampling point located with its GPS position, the corresponding pixel value was extracted for each spectral band using the point sampling tool plugin in the Quantum GIS software (QGIS).

Using the polygons of habitats identified in 2012 and 2013, we extracted vegetation points separated by 2 m from each other and placed at a minimum distance of 5 m from the border of the polygon. These points were used to test the accuracy of the final map of halophilous scrubs on an independent sample. A total of 2 653 points with 162 *A. macrostachyum* and 131 *S. fruticosa* (Table A.2) were established.

Field reflectance measurements were also collected in September 2016 using a JAZ EL 350 VIS-NIR spectrometer (350-1000 nm) from Ocean optics with a QP600-2-VIS-NIR optical fiber (600 core diameter, 24 cm bend and 12 cm radius) over 3 homogenous and dense stands of *A. macrostachyum* and 3 of *S. fruticosa*. Reflectance was registered as continuous values and averages from the 3 acquisitions were made for each species.

2.4 Mapping of halophilous scrub species distribution

The presence of halophilous scrubs was mapped using a Worldview 2 (WV2) very-high resolution imagery (Fig. 1). This sensor offered 0.46 m resolution panchromatic data (450-700 nm) and 1.85 m in multispectral, delivered at 0.5 m and 2 m, in 8 bands: B1(400-450 nm), B2 (450-510 nm), B3 (510-580 nm), B4 (585-625 nm), B5 (630 -690 nm), B6 (705-745 nm), B7 (770-895 nm) and B8 (860-1040 nm; see sensors details in Table B.1). One image was acquired the 31st of August 2016, strictly cloudless, at the time of the year when the global vegetation coverage was estimated to be at its maximum growth. The image covers the entire study area and was delivered in Ortho Ready (Final) level of correction. Multispectral indices (Table B.2), among the most used, were adapted to the bands of WV2 following the method of Davranche et al. (2010; 2013) and integrated in the database.

The Random Forest model (RF) package in the R software (Breiman, 2001) was used to perform image classification. The RF classification algorithm does not work well for unbalanced samples (Freeman et al., 2012). The class “presence of halophilous scrubs” represented 12% of the total observations. Hence, we used the function ROSE (Lunardon et al., 2014) from the R package ROSE (with $hmult.majo = 0.20$ and $hmult.mino = 0.5$) to balance our sample. We first classified both species together, *A. macrostachyum*; and *S. fruticosa*, then each species individually. For each analysis, we used a 10-fold cross validation to estimate the Out-Of-Bag (OOB) error of the classification (Breiman, 2001). The number of trees to build was set according to the best OOB score (Breiman, 2001). The final map was then validated with data from vegetation presence and absence (other land cover types) data collected in 2012 and 2013.

2.5 Flooding duration data

In this study, flooding duration is defined as the cumulated water presence based on all cloudless Sentinel 2 images available in 2016. There were a total of 15 acquisitions from February to December, corresponding to

the following dates (day/month): 05/02, 05/05, 15/05, 07/06, 07/07, 17/07, 03/08, 13/08, 26/08, 02/09, 05/09, 22/09, 05/10, 15/10, 11/12. Water presence on each date was estimated by applying the Water Index in Wetland (WIW) (Lefebvre et al., 2019) to the Sentinel-2 images level A2. The WIW can predict the presence of water irrespective of vegetation presence (Lefebvre et al., 2019). It was developed following a classification and regression tree (CART) algorithm used to identify the best match between ground-truth and optical-based data for predicting water presence/absence (Lefebvre et al., 2019). The resultant classifier of water presence consists of threshold values imposed to the near-infrared and shortwave infrared wavelengths, irrespective of the satellite sensor used (LANDSAT 5,7,8 and SENTINEL 2). The WIW provided an overall accuracy ranging from 89% to 94% for both the training and validation samples (Lefebvre et al., 2019). The highest performance was obtained for Sentinel 2 with a kappa coefficient of 0.82 (Lefebvre et al., 2019). The application of the WIW to one image results in a water map (presenting absence (coded 0) and presence (coded 1) from 2 cm of water level (Dayanche et al., 2010). Flooding duration can be obtained by the addition of all WIW rasters calculated for each acquisition date. In our case, we summed the 15 rasters corresponding to the 15 acquisition dates of cloudless images in 2016 for our study area. It provided a flooding duration (Fig. 3) ranging from 0 (always dry) to 15 (always flooded).

2.6 Sediment data

Sediment samples were collected in the summer of 2017. To track the sediment deposition and distribution changes since 2010, we collected the upper 2 cm sediment layer following fieldwork tracks defined in a GIS point layer designed with the QGIS software. The points were placed in a regular grid within the extent of the study area that was specified by a 500-m spacing between the points. The sampling points were then GPS (Garmin Etrex) referenced. Sampling points located in lagoons were discarded, but additional points were sampled in narrow water channels and in the most accessible zones. A total of 396 points were sampled (Fig. 3).

Grain size analysis of the collected sediment samples was conducted using a Malvern Mastersizer 2000© laser beam grain sizer (Parsons, 1998; Yu et al., 2009). Sand, silt and clay particle content, with their sub-groups (from very coarse to very fine fractions), and the mud estimation (sum of the silt and clay fractions) were extracted according to the Blott & Pye classification using the Excel Gradistat package (Blott and Pye, 2001). Each sample was characterized by its mean, sorting, skewness and kurtosis indexes (from the Folk

and Ward method (Folk and Ward, 1957)), with determination of their statistical mode and quantiles (median, quartiles and deciles), to evaluate its textural group (Pouzet and Maanan, 2020). Variable names are presented in Table C.1. The median grain size (d50 in μm) at each sample location was then interpolated over the entire study area. Interpolation was made with the SAGA-GIS (Conrad et al., 2015) software (version 7.9.0). Several interpolation methods were tested. To select the best method, we calculated the 10-fold cross validation error for each method. The best result was then selected according to its minimum cross validation errors (Liang et al., 2020). The cell size of the resultant interpolation raster was set to 10 m to correspond to Sentinel 2 data resolution. The resultant interpolation map was then categorized following the nomenclature of Blott and Pye (2001).

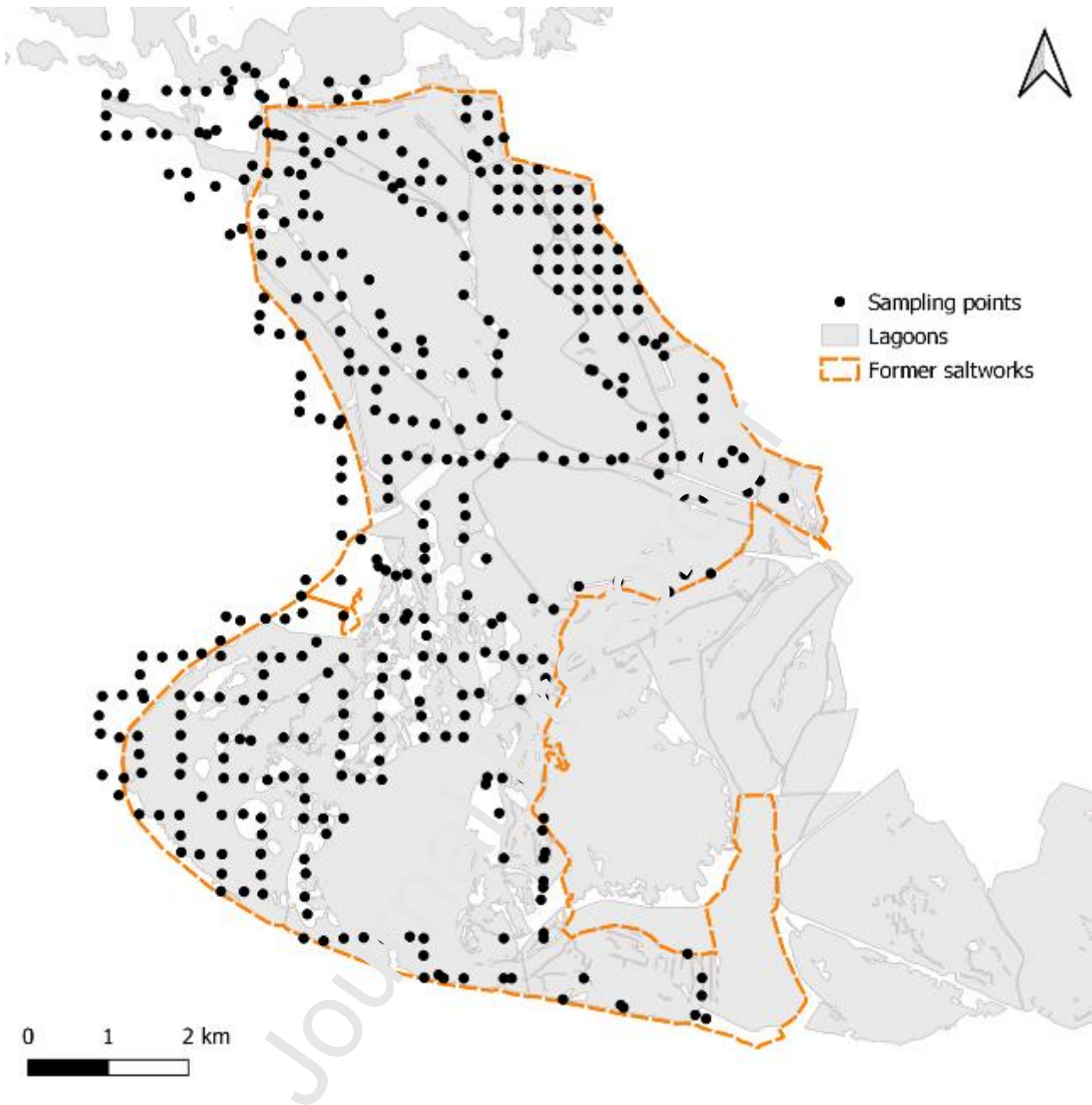


Fig. 3. Location of the sediment sampling points in the former saltworks.

2.7 Bed elevation data

Complementary, airborne topo-bathymetric LIDAR data was acquired using a Teledyne Optech Titan dual wavelength sensor using two lasers, i.e. a traditional 1064 nm for topographic acquisition, and a 532 nm (green) laser for shallow bathymetry and topography (Launeau et al., 2018; Lague and Feldmann, 2020). The airborne campaign was conducted at an altitude of 350 m on 26-27 September 2016. The ground point density was on average 15.5 pts/m² for each channel. After automated ground classification, the data was

gridded to create a 50 cm Digital Terrain Model (DTM) with a vertical accuracy for bathymetry of ± 10 cm, and for topography of ± 5 cm.

2.8 Extraction of matches between sediment samples, flooding duration, elevation and halophilous scrubs

For each sediment sampling point, we used the “point sampling tool” plugin of the QGIS software to extract the corresponding flooding duration and elevation information. Then, we defined a buffer area of 5 m distance from the points locating the sediment samples and extracted all pixels from the RF map coding for halophilous scrub presence in this zone. Halophilous scrubs were considered present at this location when there was at least one pixel coding for presence in the 5 m radius zone around each point. This approach was thought to optimize the detection of halophilous scrubs at the sampling locations of sediment records, since the point sampling tool may miss the emergence of new vegetation stands and/or sparse developments. To compare the elevation and flooding duration conditions of both species and on both sides of the main dyke that limits the marine influence, the centroids of the pixels designating the presence of each species were translated into 816 521 points. Then, using these points, the value of elevation and flooding duration were extracted for each point with the point sampling tool plugin. Finally, we created a layer of points distributed over the study area following a stratified method with a minimum distance between points of 20 meters. Based on this established grid and using the point sampling tool plugin of QGIS, we could extract 231 670 correspondences between flooding duration and the elevation values from the LIDAR DTM, irrespective of land cover types.

2.9 Statistical analyses

2.9.1 Sediment grain size parameters and halophilous scrub distribution

The Boruta package (Kursa et al., 2010) was employed to select the important predictive variables with respect to our dependent variables: flooding duration and vegetation presence. We used the TentativeRoughFix function of Boruta to get the most important shadow features (Kursa et al., 2010). Only variables with a Pearson correlation value below 0.6 were included in the same model to prevent multicollinearity (Menard, 2002). The selected variables were then used for regression model building after scaling. Since flooding duration contained 18.6% of zero values and considering under and over dispersion, we used negative binomial models and Zero-Inflated Negative Binomial GLM. Presence and absence of

halophilous scrubs were modelled using the binomial GLM with a logit link after a rebalancing process with the function ROSE (with $hmult.majo = 0.20$ and $hmult.mino = 0.50$) of the R package ROSE (Lunardon et al., 2014) since the category “presence of halophilous scrubs” was representing 12% of the total observations. Our objective was to find the best predictive model. Hence, the dredge function of the Mumin R package was used to identify the top model (within a range of $\Delta AIC \leq 2$). Resultant model selection was conducted using minimum AIC value and evaluation of residuals with the DHARMA package.

2.9.2 Elevation and flooding duration and halophilous scrub distribution

Elevation values followed a non-normal distribution (Shapiro-Wilk test, $p=0.001$). Hence, we performed pairwise *Kruskall-Wallis* tests with bonferroni adjusted P-values (threshold of $p=0.025$, for 15 categories) to compare elevation means of each category of flooding duration (0 = dry to 15 = 15 dates of water presence) using the agricolae R package. The distribution of halophilous scrub species on both sides of the seafront dyke were compared in relation to the flooding duration considered as a continuous variable (Shapiro-Wilk test $p < 0.001$); using the agricolae R package, pairwise *Kruskall-Wallis* tests compared the mean flooding duration for both species on both sides of the backward dyke (to the North and to the South).

3. Results

3.1 Spectral characteristics and classification accuracy of halophilous scrub presence (RF)

Field measurements of reflectance of *S. fruticosa* and *A. macrostachyum* provided different spectral curves: the absorption in the red light was greater for *S. fruticosa* and its reflectance values in the near-infrared (NIR) part of the spectrum was higher than for *A. macrostachyum* (Fig. 4). The point when *A. macrostachyum* reflectance values decreased compared to *S. fruticosa* was at about 710 nm.

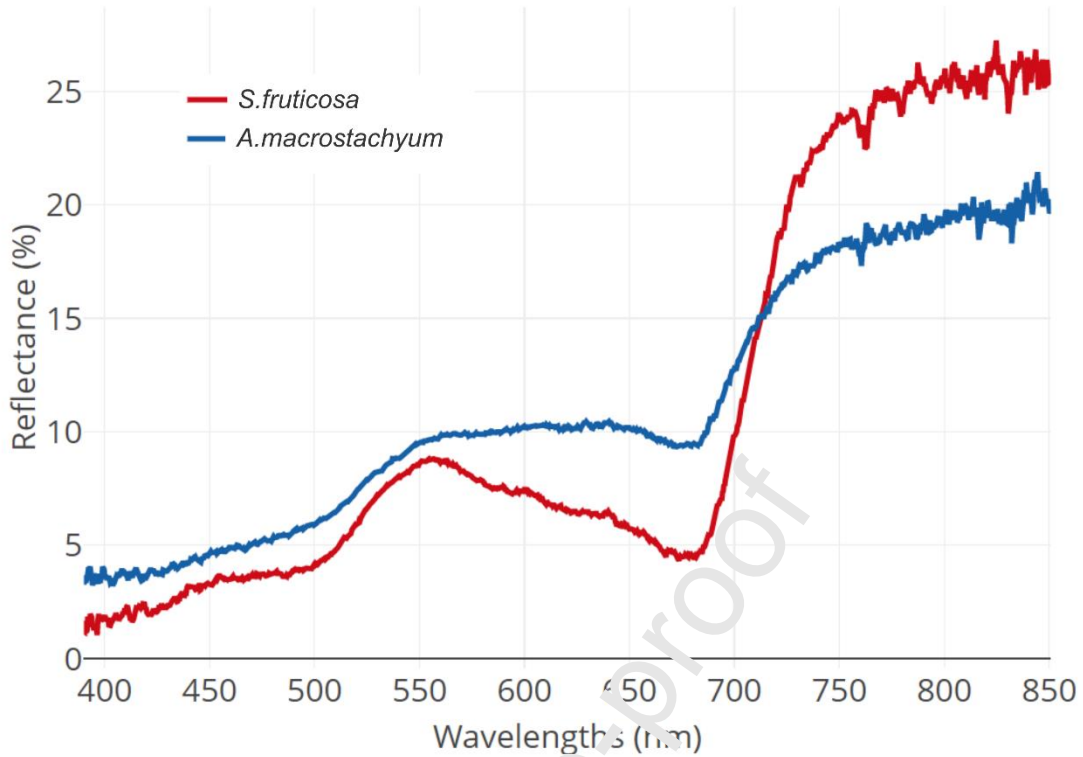


Fig. 4. Reflectance of *S. fruticosa* and *A. macrostachyum*, measured with a Jaz spectrometer in the field on 7-8 September 2016.

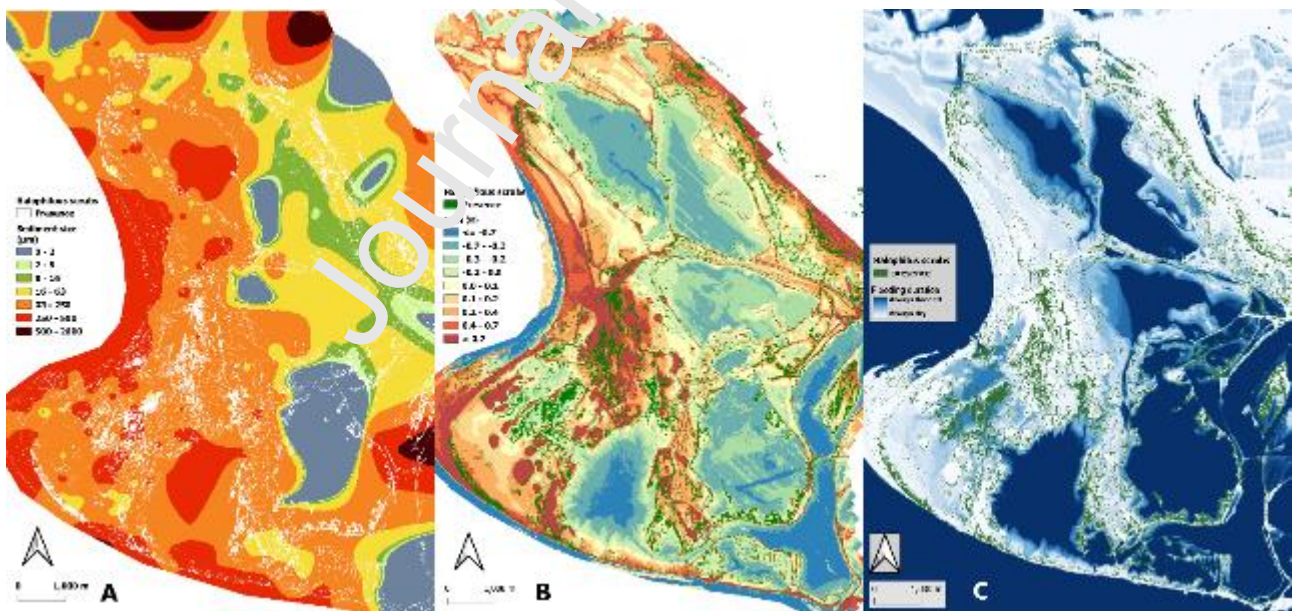
RF OOB and omission errors for class “presence” and the class “absence” were less important when the classification (Davranche et al, 2023) was done for each species individually than for both species together (Table 1). For both species, the most discriminant variable was the NDVI2 according to the mean decrease Gini (see supplementary material S1), which is a measure of node impurity (Breiman, 2001). The validation on the independent sample from data collected from 2010 to 2013 provided an omission error of 27% for *A. macrostachyum* and 44% for *S. fruticosa* with a global accuracy of 96.2% (Appendice B).

Table 1: RF error estimates on the training sample

	OOB error (%)	Omission error presence (%)	Omission error absence (%)
	Sample 2016	Sample 2010 to 2013	Sample 2010 to 2013
<i>S. fruticosa</i>	1.43	0.017	0.012
<i>A. macrostachyum</i>	2.18	0.025	0.019
Both species	6.08	0.064	0.057

3.2 Sediment grain size distribution

According to the cross-validation error, the best method for the D50mm interpolation (Davranche et al., 2023b) was the Modified Quadratic Shepard. The 10-fold validation provided an R^2 of 0.93, an NMRSE of 24.5, an RMSE of 83.9, an MRE of 7039 with the fit set to “node”, the quadratic neighbours and weighting neighbours set to 50 and the spatial resolution set to 10 m equivalent to the Sentinel 2 image resolution (Fig. 5A). The combination of all maps (Fig. 5) highlights several circular, higher and dry structures of different surfaces, made up of a mix of coarse and fine sediments in the western and southern parts of the site. Halophilous scrubs can be seen around these spherical structures, especially to the South, along the former seafront dyke breaches, and to the West along the coast (Animation on Fig. 5D). The Eastern lagoon basins, close to the former Rhône River pathway, exhibit the finest sediments ($D_{50mm} < 63 \mu m$, Fig. 5A). Zones with very coarse sediments join the sea to South and West, especially where dyke breaches are present (Fig. 5A).



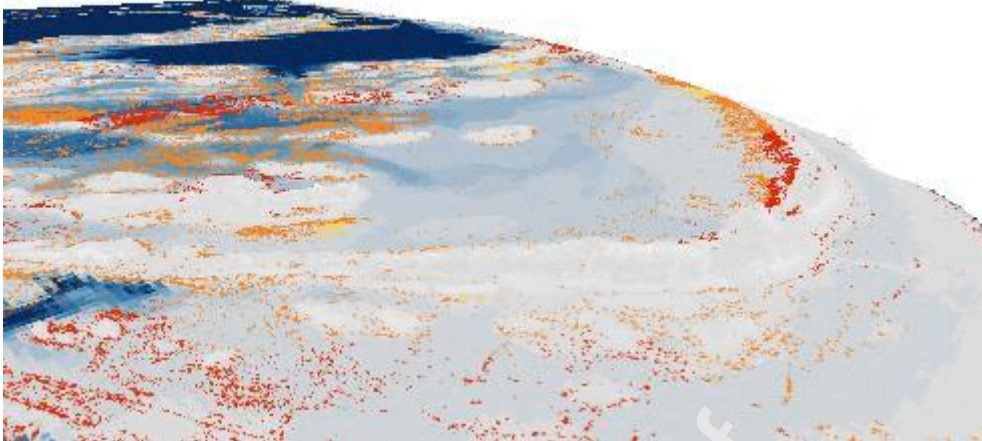


Fig. 5. Classification (spatial resolution 2 m) of perennial halophilous scrubs (*S. fruticosa* and *A. macrostachyum*) placed on (A) the interpolation of median grain size (D50mm; discretization based on quantile, spatial resolution 10 m), (B) the DTM (spatial resolution 50 cm; discretization based on quantiles) and (C) the flooding duration from 0 (always dry) to 15 (always flooded) (spatial resolution = 10) in the former saltworks of Salin de Giraud. (D) is a 3D animation starting from North-West and finishing South-East, based on a set of camera positions placed on the combination of the 3 maps; the median grain size was extracted for each pixel of halophilous scrubs placed on the flooding duration map shaped with the DTM in three dimensions (vertical scale = 4, tile resolution = 200 px, skirt height = 1, offset = 1).

3.2.1 Prediction of halophilous scrub distribution with sediment size parameters

After Boruta and Pearson correlation testing, the pre-selected variables were D10mm and VFINESILT (Table 2). The resultant model followed a binomial logit distribution. The Area Under the Curve (AUC) of the Receiver Operator Characteristic (ROC) curve was 0.65 (it can range from 0 to 1). The model shows that halophilous scrubs from *S. fruticosa* and *A. macrostachyum* developed on coarser sediments rather than finer particles (negative slope).

Table 2: Resultant model predicting halophilous scrubs occurrence with sediment size parameters

Model type	Response variable	Predictive variables	Estimates	Error	P
Logit	Presence of halophilous scrubs	Intercept	-2.588	0.223	0

		D10mm	-0.657	0.303	0.03
		VFINESILT	-0.631	0.281	0.02

3.2.2 Prediction of flooding duration with sediment size parameters

After Boruta and Pearson correlation testing, the pre-selected variables were VCOARSESTILT, COARSESTAND and CLAY. The best predictive model followed a negative binomial distribution, showing an increasing percentage of CLAY with flooding duration, an inverse relation to VCOARSESTILT size, and a negative relation of water absence with COARSESTAND and VCOARSESTILT. P values were more significant for flooding duration than for water absence (flooding duration = 0, Table 3). It means that long hydroperiods will be observed in zones where the proportion of clay is greater, and the proportion of very coarse silt is less important. It also means that the presence of water, irrespective of the hydroperiod, can be observed in areas with a higher proportion of coarse sand and coarse silt.

The map of flooding duration over the 15 dates in 2010 highlights the largest lagoons on the Eastern part of the study area with their deepest areas that are permanently flooded. It also highlights the water pathways between the lagoons and the channels created by the regular sea inflow (Fig. 5C).

Table 3: Resultant models predicting flooding duration and water presence with varying sediment size parameters

Model type	Response variable	Predictive variables	Estimates	Error	P
Negative binomial	Flooding duration	Intercept	1.353	0.051	0
		CLAY	0.265	0.060	0
		VCOARSESTILT	-0.359	0.066	0
		Log(theta)	0.429	0.116	0
Zero-inflation model, binomial with logit link	Water absence	Intercept	-15.887	7.663	0.038
		COARSESTAND	-1.636	0.804	0.042
		VCOARSESTILT	-11.761	5.802	0.043

3.3 Halophilous scrub distribution related to elevation and flooding duration

According to the random forest map, both species of halophilous scrubs are distributed in higher mean elevations to the North of the backward dyke than to the South (higher marine influence). On both sides of the backward dyke, *A. macrostachyum* is located at lower mean elevations (northeast= 0.45 m, southwest: 4.1 m) than *S. fruticosa* (northeast: 0.60 m, southwest: 0.78 m). In the southern part of the study area, where the topographical variation is higher in the elevation model, *S. fruticosa* and *A. macrostachyum* can be found at larger ranges of elevation values than in the Northern part. The species can be found at significant different elevation means on both sides of the backward dyke (see letters on Fig. 6).

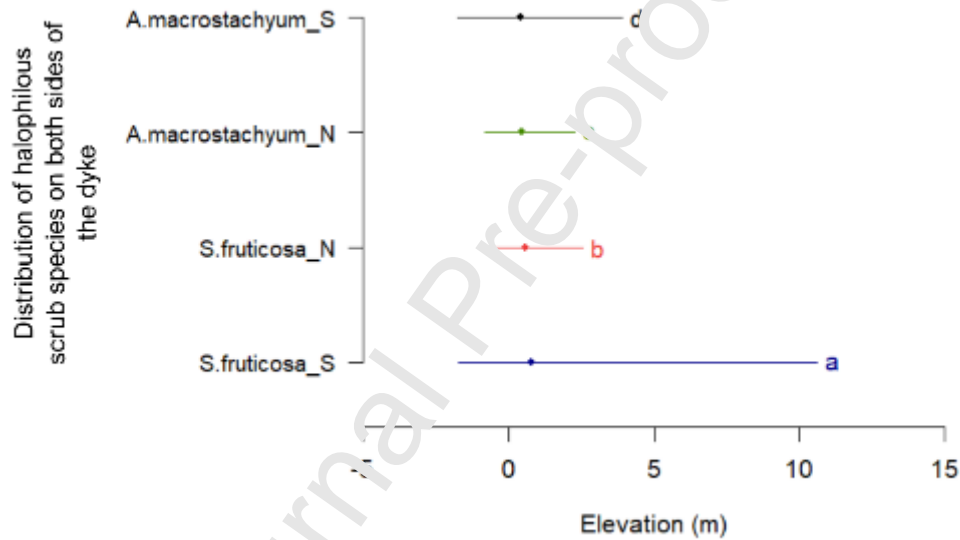


Fig. 6: Comparison of mean elevation of both species on both sides of the backward dyke (*S.fruticosa*_N = *S. fruticosa* northeast of the dyke, *S.fruticosa*_S = *S. fruticosa* southwest of the dyke; *A.macrostachyum*_N = *A. macrostachyum* northeast of the dyke, *A.macrostachyum*_S = *A. macrostachyum* southwest of the dyke), bars representing the range of elevation values from minimum to maximum where species can be found according to the random forest classification. The different letters (a, b, c, d) mean that the mean values are significantly different from each other.

According to the random forest classification, both species on both sides of the backward dyke can be found where duration of flooding ranges from none to all fifteen dates but their distribution configurations differed significantly in terms of mean flooding duration. Overall, *A. macrostachyum* experienced longer inundation (northeast: 0.7 dates, southwest: 3.2 dates) than *S. fruticosa* (northeast: 0.5 dates, southwest: 2.3 dates), and

longer inundation in the southern part than in the northern part of the study area. *S. fruticosa* also experienced longer inundation in the southern part of the study area that is directly influenced by the sea (Fig. 7).

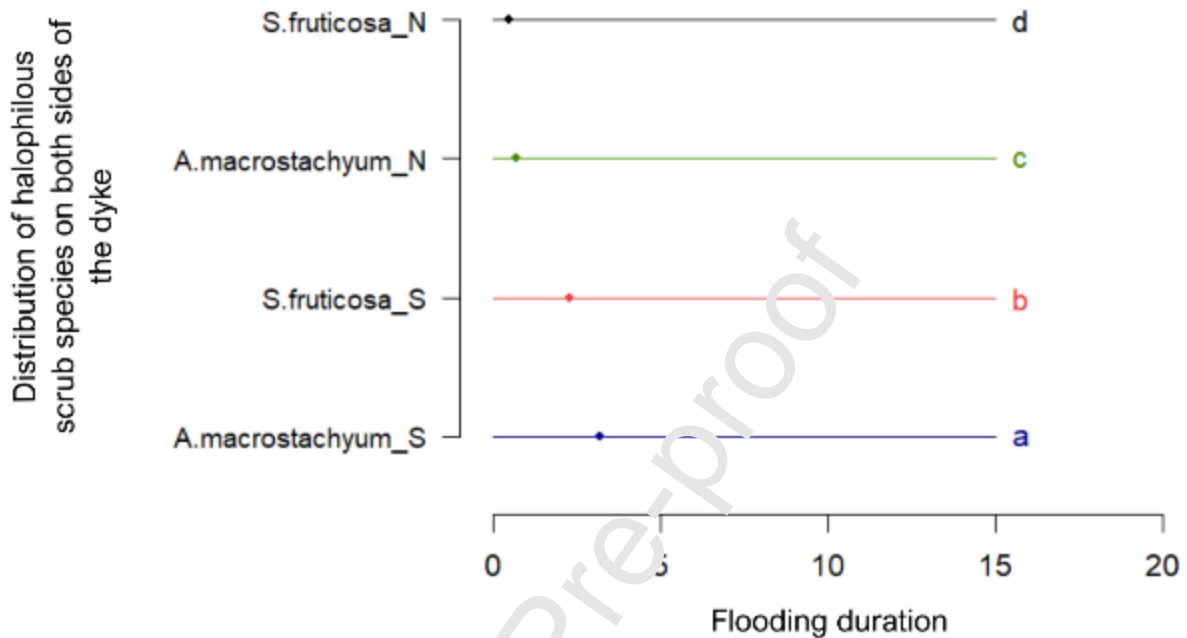


Fig. 7. Comparison of mean flooding duration of both species on both sides of the backward dyke (*S. fruticosa*_N = *S. fruticosa* northeast of the dyke, *S. fruticosa*_S = *S. fruticosa* southwest of the dyke; *A. macrostachyum*_N = *A. macrostachyum* northeast of the dyke, *A. macrostachyum*_S = *A. macrostachyum* southwest of the dyke), bars representing the range of flooding duration from minimum to maximum (0 to 15) where species can be found according to the random forest classification. The different letters (a, b, c, d) identify mean values that are significantly different from each other.

3.4 Flooding duration distribution related to elevation

The pairwise comparisons of mean elevation and flooding duration categories showed that dry zones (0 date), rarely inundated zones (1 date), and mid-dry zones (up to 7 dates of flooding) are located at a significantly different altitude than areas being flooded more than 50% of the time. The longest hydroperiods (all 15 dates) are observed in the deepest zones having the lowest mean elevation (one single group called “m” on Fig. 8), ranging from -12,7 meters to 1,6 meters.

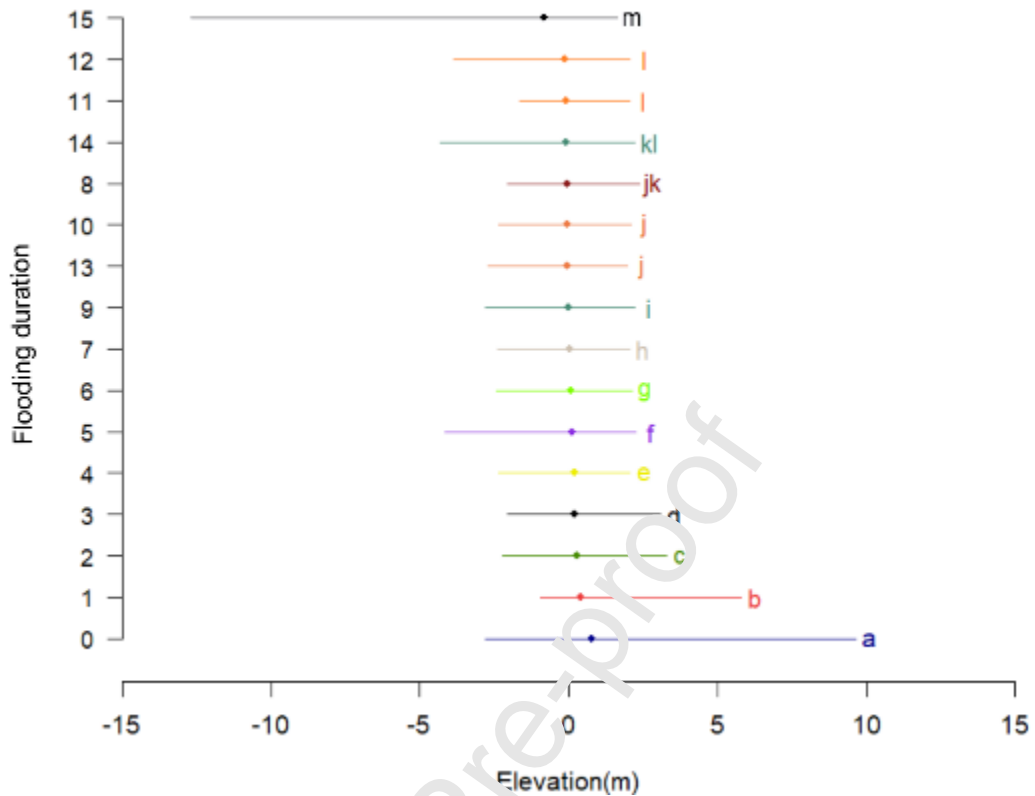


Fig. 8. Flooding duration (duration from 0 to 15 days) grouped and ranked according to the pairwise analysis with *Kruskal-Wallis* test and bonferroni *p* adjustment of their mean values of elevation on the DTM (a to h letters are group identifiers (different group - significant difference), bars are range values (min-max)).

4. Discussion

4.1. Halophilous scrub distribution mapping

The reflectance measured with a field spectrometer showed that the *A. macrostachyum* spectral curve in the yellow band of WV slightly overlaps with the green band. Compared to *S. fruticosa*, the reflectance value in the green light is slightly over the yellow and red, most likely due to the physiognomic difference when *A. macrostachyum* segments turn yellow-brown, *S. fruticosa* remains green (Davy et al., 2006). The difference in spectral responses was confirmed with the classification accuracies from WV2 data (improved accuracies for classification when the species are considered separately). As stated by several previous studies (Ali et al., 2016; Rapinel et al., 2019; Vanden Borre et al., 2011), this result confirms that field experts and conservation site managers must work together on data standardization and knowledge sharing for improving the use of remote sensing to fulfil Natura 2000 habitat monitoring. This result has important implications in

terms of field protocol for the mapping of these species that are grouped under the same category “halophilous scrubs” in the Natura 2000 typology. Our field protocol specifications could be applied in other areas for future mapping of coastal marsh vegetation.

Mapping of both species was mostly linked to the NDVI2 multispectral index. The NDVI2 calculated from WV2 bands can improve vegetation biomass mapping at high density (Mutanga et al., 2012). Since homogeneous stands of halophilous scrubs can be very dense in our study site, it may explain the importance of this variable for mapping this Natura 2000 habitat. Regarding mapping costs, a single image of WV2 for one date was found sufficient to build an accurate map of both species' distribution. The validation on an independent sample provided a good overall accuracy for both species. This validation shows that other land cover types, habitats and species are well identified as “absence of halophilous scrubs”. However, results showed an underestimation of the presence of both species, especially *S. fruticosa* (omission error 44%). The validation sample was made with data acquired from 2010 to 2013 according to the identification of Natura 2000 habitats with no assurance that the stands of *A. racrostachyum* and *S. fruticosa* were in the same ecological state in 2016. Also, cover percentages were not specified in the available database and sampling points placed in the polygons could fall on very sparsely vegetated areas. Some of them might have been placed on bare soil or on a mix of halophilous scrubs with other species that might partly explain the error of omissions with this validation sample. Also, further investigations must be conducted on the development of *S. fruticosa* that might mix with other species such as *Juncus maritimus* as observed in the field (expert knowledge from Tour du Val, unpublished), which could further explain the omission error if both species can mix at equal proportion. However, regarding the OBB errors resulting from the random forest algorithm, the classification can be considered accurate for both species, since this method was proven to be a reliable measure of classification accuracy (Lawrence et al., 2006; Zhong et al., 2014). Hence, our study adds elements to the conclusions of Vanden Borre et al. (2011) regarding the suitability of Natura 2000 typology for remote sensing data i.e. vegetation stand homogeneity is not a prime descriptive parameter of the Natura 2000 typology. This study confirms that rigorous field campaigns combined with satellite remote sensing can provide models for vegetation presence (Davranche et al., 2010; Lefebvre et al., 2019) if the protocol to build a sample for remote sensing analysis is made in accordance with the resolution of the

image. These results confirmed the need for protocol standardization between field experts and remote sensing analysts (Vanden Borre et al., 2011).

4.2. Halophilous scrubs, flooding duration and elevation

Generally, our resultant map of halophilous scrubs presence follows the highest elevation variability in the northern part of our study zone (i.e., to the North of the backward dyke) compared to the southern part. According to this map, *S. fruticosa* seems to be distributed at a higher mean elevation and in mean shorter duration flooded zones than *A. macrostachyum*. However, the range of values suggests that *A. macrostachyum* can be found in diverse flooding conditions, and in some places, at higher elevations than *S. fruticosa*. While providing a synoptic view of the whole study area, our map seems to follow the observations of Molinier and Tallon (1965). They explained that *A. macrostachyum* can be observed at very low elevations (lower than *S. fruticosa*) and in areas exhibiting longer flooding durations, which it can withstand better than *S. fruticosa*, or at higher elevations under higher salinity pressure, both conditions inducing phenotypic adaptations of *A. macrostachyum*. They also showed that *A. macrostachyum* can participate in the edification of mobile embryonic dunes. *A. macrostachyum* can also be seen in mix stands with annual glasswort in salty steppes, as noticed in the Tour du Valat inventories from 2010 to 2013 (Conservatoire du Littoral, 2015). These observations seem to confirm the accuracy of our mapping approach. When considering the mean values of flooding duration for each species, it seems that both species can more often be seen in zones that were flooded for about 1 date over the 15 dates we monitored. Our model predicting flooding duration with sediment size showed that the less flooding duration the less the sediments are coarse. Both species seems to develop preferably on coarser sand and silt. According to our map, although distributed on a larger range of elevations in the southern part of the study area, *S. fruticosa* seems to generally develop at higher altitudes than *A. macrostachyum* in this zone that is directly influenced by the sea inflows, especially since the seafront dyke started collapsing. Sea water inflows might favour *A. macrostachyum* at lower elevations because it is less sensitive to high variability (Rogel et al., 2000). However, the presence of halophilous scrubs could not be predicted by the flooding duration extracted from SENTINEL data or by elevation. Further investigations are required to model the percent coverage of halophilous scrubs rather than their occurrences. As stated by studies conducted along an inundation gradient (Khan and Gul, 2002), we might expect the cover of *A. macrostachyum* to be lower in zones that receive the

maximum inundation. Field data gathering, including percentage cover of the vegetation stands should be further undertaken to test this hypothesis.

4.3. Halophilous scrub occurrence and sediment grain size distribution

Results of our model, linking the halophilous scrub distribution map and sediment sizes, confirmed previous deductions regarding the flooding duration category where this vegetation develops. The presence of halophilous scrubs is negatively correlated to very fine particles of silt. Areas of smaller grain sizes at higher elevations (embryonic dunes) can be seen to the South in the interpolation map of the sediment median size, and they are surrounded by halophilous scrub development. The sea seems to import coarser sediments on which the halophilous scrubs develop, after which they then retain the finer sediments. These observations support the identifications of dunes by the managers of the site who suggested the contribution of halophilous scrub to the formation of these dunes (Parc naturel régional de Camargue et al., 2022). The application of our method might help to identify areas where vegetation develops and new dunes are likely to develop, starting with the first deposition of sediment.

4.4 Adaptive management to cope with sea-level rise

Climate change scenarios suggested that a small increase in storms (energy and duration) would result in increased dune erosion in Camargue (Sabatier, 2008). The renaturation process, by restoring seasonal water cycles, has allowed halophilous scrubs to develop on mud flats, further contributing to sediment trapping and dune formation. The collapse of the seafront dyke has resulted in the restoration of coastal dynamics. Climate scenarios (Sabatier, 2008) did not take into account this renaturation process of lagoons. This process limits human activities that reduce or eliminate forcings such as major storm events and river floods at different temporal and spatial scales (Day et al., 2011). These forcings are known to cause wetland losses and sediment inflow modifications (Day et al., 2011). Our results confirmed that unhindered sea inflow had, at least locally, a short-term positive impact on the development of halophilous vegetation and dune formation, as observed by the site managers (Parc naturel régional de Camargue, Tour du Valat, Société nationale de protection de la nature & CPIE Rhône Pays d'Arles, 2022).

In 2010, Day et al. (2010) studied several Mediterranean deltaic and lagoon wetlands including the Eastern part of the Rhône River delta. They concluded that areas with high riverine sediment inflow are the only ones

likely to survive to the accelerated sea-level rise. They explained that impounded marshes, isolated from both tidal and river influence, had low biomass and mineral sediment inflows, and were losing elevation relative to local water levels. In the Rhône River delta, they observed that the hypersaline soil was an additional stress impacting negatively on plant production to offset elevation loss. However, our results suggested that the nature-based restoration process applied to the former saltworks of Salin de Giraud at least partially compensate the lack of river sediment inflows. The halophilous scrub emergence in the southwestern part of our study site could be predicted by the presence of coarser sediments brought in by the sea. Halophilous scrubs seem to create a basis for sediment accumulation that foster the formation of new dunes. The storm frequency and the impact of wind on sea inflow into this very flat region might contribute to the specific distribution of halophilous scrub species observed in our study site by contributing to the edaphic conditions needed for their development..

The adaptive management process applied to our study area has been implemented through a nature-based solution approach with restoration of gravitational water flows and abandonment of seafront dykes that resulted in the creation of a natural littoral environment (Conservatoire du Littoral, 2015). Simulations showed that the salt marsh habitats in the northern part of the Venice lagoon will disappear by 2075 because the anthropogenic barriers are limiting the sediment availability to all micro-altitudes (Ivajnsič et al., 2018). The synoptic view brought by our approach could help developing adaptive management strategies in such lagoons to decrease the impact of humans and favour sediment deposition following the emergence of marsh vegetation as observed in our study area.

4.5 Applicability of the approach to other areas

In this study, we presented two models linking vegetation development and flooding duration mapped with remote sensing with sediment size distribution. Derived data from remote sensing can therefore help to understand the dynamics of the edaphic characteristics needed for salt marsh species development. It offers perspectives for long-term and regular monitoring strategies of nature-based solutions over large areas with limited sediment sampling and analyses required. Our results showed that vegetation mapping at one date can be used to understand mid-term (in this study 6 years, from 2010 to 2016) sediment dynamics of Mediterranean lagoons facing global change. In our study, the monitoring was done after a period of high anthropogenic impact. However, it can be applied to other saltwork regions to better understand the impact

of such human activities and to better regulate them. Our study area is very flat, but the LIDAR data provided bathymetry up to -13 meters under the water surface close to the border of the beach in the sea. This approach offers great potential to apply the approach in coastal regions where the topography and depths are important drivers. According to our results, in very, flat micro-intertidal areas, like the Salins de Giraud, multispectral indices, such as the WIW, seems to be helpful in understanding the water pathways and their impact on vegetation development related to sediment grain size. Hence, the high acquisition periodicity of SENTINEL images offers a useful tool to understand the impact of extreme storm water inflow in the process of sea-level rise, since it can highlight and assist in measuring the surfaces that are rarely inundated. In this study, we considered flooding duration using one or two images monthly but the constellation of SENTINEL 2 with a third satellite to be launched in 2024, will increase the temporal resolution. It will help to better understand the impact of sea inflow on vegetation development and sediment dynamics in coastal areas.

Conclusion

The former saltworks of Salin de Giraud in Camargue, purchased by the Conservatoire du Littoral in 2010, offered a unique landscape configuration in France to test the relevance of remote sensing approaches based on World view 2, SENTINEL 2 and a full wave LIDAR sensor to monitor the nature-based restoration of a coastal area exposed to sea-level rise. Our interdisciplinary approach demonstrated that derived data from remote sensing linked to grain size analysis of sediments, can help to understand the distribution, the emergence and stand development of salt marsh vegetation species by imaging the edaphic conditions from space and in the field. Remote y-sensed data on water presence could also be explained by the grain size, while the LIDAR elevation did not seem to be a significant parameter of flooding duration or sediment distribution in our study area. This might be due to the very flat topography that is rapidly changing with sea inflows. Our results suggested that remote sensing of water and vegetation presence related to the sediment distribution can help with assessing the effectiveness of an adaptive management strategy based on a renaturation process of lagoons highly pressured by anthropogenic activities. Field campaigns to monitor vegetation development over large areas are costly, especially in time, which hinders the possibility to cover the entire study area before it evolved further with climate change. In the context of the increased availability of time series imagery, our synoptic approach offers new possibilities for managers to better define adaptive

strategies, increased uptake in governance programs, for the restoration of coastal areas and to facilitate the monitoring of these nature-based solutions at larger scales.

Acknowledgments:

Funding was provided by the Agence de l'eau RMC and the MAVA Foundation. Aurélie Davranche was supported by the CNRS and the University of Angers for three 6-months research leaves. The Teledyne Optech Titan DW LIDAR sensor used in this study is operated by the Nantes-Rennes Topo-Bathymetric lidar platform (University of Rennes 1/University of Nantes) and has been funded by the Region Pays de la Loire with funding of the RS2E-OSUNA programs and the Region Bretagne with support from the European Regional Development Fund. The Camargue reserve provided access for field sampling. A. Rita Carrasco was supported by the contract DL57/2016/CP1361/CTC002. A. Rita Carrasco and Alice Newton acknowledge LA/P/0069/2020 and UID/00350/2020 CIMA, all funded by Fundação para a Ciência e Tecnologia. Alice Newton acknowledges Future Earth Coasts. Céline Arzel received a grant from the Academy of Finland (grant number 333400).

Data availability statement

The Sentinel 2 images used to calculate the flooding duration were value-added data processed by the CNES for the Theia www.theia.land.fr data cluster using Copernicus data. The treatments use algorithms developed by Theia's Scientific Expertise Centres. The LIDAR DTM and the sediment sampling database are available from the corresponding author upon request. The rasters of halophilous scrub distribution in 2016 and the interpolation of median sediment grain size were shared online (see DOI provided in the reference list).

References

- Abdulrahman, F.S., Williams, G.J., 1981. Temperature and salinity regulation of growth and gas exchange of *Salicornia fruticosa* (L.) L. *Oecologia* 48, 346–352. <https://doi.org/10.1007/BF00346493>
- Ali, I., Cawkwell, F., Dwyer, E., Barrett, B., Green, S., 2016. Satellite remote sensing of grasslands: from observation to management. *Journal of Plant Ecology* 9, 649–671. <https://doi.org/10.1093/jpe/rtw005>

- Aubert, B., Boudet, G., Lacassin, J.-C., Legros, J.-P., 2023. Les terres de Camargue dans leur environnement. *Étude et Gestion des Sols* 30, 263–265. https://www.afes.fr/wp-content/uploads/2023/03/EGS_2023_30_Aubert_263-286.pdf
- Baumberger, T., Affre, L., Croze, T., Mesléard, F., 2012. Habitat requirements and population structure of the rare endangered *Limonium girardianum* in Mediterranean salt marshes. *Flora - Morphology, Distribution, Functional Ecology of Plants* 207, 283–293. <https://doi.org/10.1016/j.flora.2011.11.008>
- Belluco, E., Camuffo, M., Ferrari, S., Modenese, L., Silvestri, S., Marani, A., Marani, M., 2006. Mapping salt-marsh vegetation by multispectral and hyperspectral remote sensing. *Remote Sensing of Environment* 105, 54–67. <https://doi.org/10.1016/j.rse.2006.06.005>
- Bioret, F., Mathevet, R., in Garnier, L., 2008. La gestion adaptative des territoires de la biodiversité in “Entre l’homme et la nature, une démarche pour des relations durables.” UNESCO Notes Techniques n°3, 74–76.
- Blott, S.J., Pye, K., 2001. GRADISTAT: a grain size distribution and statistics package for the analysis of unconsolidated sediments. *Earth Surface Processes and Landforms* 26, 1237–1248. <https://doi.org/10.1002/esp.261>
- Blount, T.R., Carrasco, A.R., Cristina, S., Silvestri, S., 2022. Exploring open-source multispectral satellite remote sensing as a tool to map long term evolution of salt marsh shorelines. *Estuarine, Coastal and Shelf Science* 266, 107664. <https://doi.org/10.1016/j.ecss.2021.107664>
- Bobbink, R., Whigham, D.F., Beltman, B., Verhoeven, J.T.A., 2006. Wetland Functioning in Relation to Biodiversity Conservation and Restoration, in: Bobbink, R., Beltman, B., Verhoeven, J.T.A., Whigham, D.F. (Eds.), *Wetlands: Functioning, Biodiversity Conservation, and Restoration, Ecological Studies*. Springer, Berlin, Heidelberg, pp. 1–12. https://doi.org/10.1007/978-3-540-33189-6_1
- Breiman, L., 2001. Random Forests. *Machine Learning* 45, 5–32. <https://doi.org/10.1023/A:1010933404324>
- Campbell, A., Wang, Y., 2019. High Spatial Resolution Remote Sensing for Salt Marsh Mapping and Change Analysis at Fire Island National Seashore. *Remote Sensing* 11, 1107. <https://doi.org/10.3390/rs11091107>
- Colmer, T.D., Flowers, T.J., 2008. Flooding tolerance in halophytes. *New Phytologist* 179, 964–974. <https://doi.org/10.1111/j.1469-8137.2008.02483.x>

- Conrad, O., Bechtel, B., Bock, M., Dietrich, H., Fischer, E., Gerlitz, L., Wehberg, J., Wichmann, V., Böhner, J., 2015. System for Automated Geoscientific Analyses (SAGA) v. 2.1.4. *Geoscientific Model Development* 8, 1991–2007. <https://doi.org/10.5194/gmd-8-1991-2015>
- Conservatoire du Littoral, 2015. Site des étangs et marais des Salins de Camargue, rapport d'activités 2015.
- Davranche, A., Lefebvre, G., Poulin, B., 2010. Wetland monitoring using classification trees and SPOT-5 seasonal time series. *Remote Sensing of Environment* 114, 552–562. <https://doi.org/10.1016/j.rse.2009.10.009>
- Davranche, A., Poulin, B., Lefebvre, G., 2013. Mapping flooding regimes in Camargue wetlands using seasonal multispectral data. *Remote Sensing of Environment* 138, 165–171. <https://doi.org/10.1016/j.rse.2013.07.015>
- Davranche A., Arzel C., Pouzet P., Carrasco A. R., Lefebvre G., Lague D., Thibault M., Newton A., Fleurant C., Maanan M., Poulin B., 2023a. Presence of perennial halophilous scrubs in 2016 in the former saltworks of Salins de Giraud, random forest classification on WV2. <https://doi.org/10.5281/zenodo.8118198>
- Davranche Aurélie, Arzel Céline, Carrasco A. Rita, Pouzet Pierre, Lefebvre Gaëtan, Lague Dimitri, Thibault Marc, Newton Alice, Fleurant Cyril, Maanan Mohamed, Poulin Brigitte, 2023b. Interpolation of the median grain size of the first 2 cm sediment layer in the former saltworks of Salin de Giraud in 2017. <https://doi.org/10.5281/zenodo.8132333>
- Day, John, Ibáñez, C., Scarton, P., Pont, D., Hensel, P., Day, Jason, Lane, R., 2011. Sustainability of Mediterranean Deltaic and Lagoon Wetlands with Sea-Level Rise: The Importance of River Input. *Estuaries and Coasts* 34, 483–493. <https://doi.org/10.1007/s12237-011-9390-x>
- El Mahrad, B., Newton, A., Icely, J.D., Kacimi, I., Abalansa, S., Snoussi, M., 2020. Contribution of Remote Sensing Technologies to a Holistic Coastal and Marine Environmental Management Framework: A Review. *Remote Sensing* 12, 2313. <https://doi.org/10.3390/rs12142313>
- Evans, D., Arvela, M., 2011. Assessment and reporting under Article 17 of the Habitats Directive.
- Fagherazzi, S., Mariotti, G., Leonardi, N., Canestrelli, A., Nardin, W., Kearney, W.S., 2020. Salt Marsh Dynamics in a Period of Accelerated Sea Level Rise. *Journal of Geophysical Research: Earth Surface* 125, e2019JF005200. <https://doi.org/10.1029/2019JF005200>

- Folk, R.L., Ward, W.C., 1957. Brazos River bar [Texas]; a study in the significance of grain size parameters. *Journal of Sedimentary Research* 27, 3–26. <https://doi.org/10.1306/74D70646-2B21-11D7-8648000102C1865D>
- Fraixedas, S., Galewski, T., Ribeiro-Lopes, S., Loh, J., Blondel, J., Fontès, H., Grillas, P., Lambret, P., Nicolas, D., Olivier, A., Geijzendorffer, I.R., 2019. Estimating biodiversity changes in the Camargue wetlands: An expert knowledge approach. *PLOS ONE* 14, e0224235. <https://doi.org/10.1371/journal.pone.0224235>
- Freeman, E.A., Moisen, G.G., Frescino, T.S., 2012. Evaluating effectiveness of down-sampling for stratified designs and unbalanced prevalence in Random Forest models of tree species distributions in Nevada. *Ecological Modelling* 233, 1–10. <https://doi.org/10.1016/j.ecolmodel.2012.03.007>
- Höhener, P., Comoretto, L., Housari, F. al, Chauvelon, P., Pichaud, M., Chérain, Y., Chiron, S., 2010. Modeling anthropogenic substances in coastal wetlands: Application to herbicides in the Camargue (France). *Environmental Modelling & Software* 25, 1837–1844. <https://doi.org/10.1016/j.envsoft.2010.05.005>
- Hu, Z., Borsje, B.W., van Belzen, J., Willemsen, P.W.J.M., Wang, H., Peng, Y., Yuan, L., De Dominicis, M., Wolf, J., Temmerman, S., Bouma, T.J., 2021. Mechanistic Modeling of Marsh Seedling Establishment Provides a Positive Outlook for Coastal Wetland Restoration Under Global Climate Change. *Geophysical Research Letters* 48, e2021GL095596. <https://doi.org/10.1029/2021GL095596>
- Ivajnsič, D., Kaligarič, M., Fantinato, E., Del Vecchio, S., Buffa, G., 2018. The fate of coastal habitats in the Venice Lagoon from the sea level rise perspective. *Applied Geography* 98, 34–42. <https://doi.org/10.1016/j.apgeog.2018.07.005>
- Khan, M.A., Gul, B., 2002. *Arthrocnemum macrostachyum*: a potential case for agriculture using above seawater salinity, in: Ahmad, R., Malik, K.A. (Eds.), *Prospects for Saline Agriculture, Tasks for Vegetation Science*. Springer Netherlands, Dordrecht, pp. 353–364. https://doi.org/10.1007/978-94-017-0067-2_37
- Kursa, M.B., Jankowski, A., Rudnicki, W.R., 2010. Boruta – A System for Feature Selection. *Fundamenta Informaticae* 101, 271–285. <https://doi.org/10.3233/FI-2010-288>
- Lague, D., Feldmann, B., 2020. Chapter 2 - Topo-bathymetric airborne LiDAR for fluvial-geomorphology analysis, in: Tarolli, P., Mudd, S.M. (Eds.), *Developments in Earth Surface Processes, Remote*

Sensing of Geomorphology. Elsevier, pp. 25–54. <https://doi.org/10.1016/B978-0-444-64177-9.00002-3>

Landi, M., Angiolini, C., 2013. Soil-Plant Relationships in Mediterranean Salt Marshes across Dune-Cultivated Land Gradient. *Journal of Coastal Research* 31, 588–594. <https://doi.org/10.2112/JCOASTRES-D-13-00009.1>

Launeau, P., Giraud, M., Ba, A., Moussaoui, S., Robin, M., Debaine, F., Lague, D., Le Menn, E., 2018. Full-Waveform LiDAR Pixel Analysis for Low-Growing Vegetation Mapping of Coastal Foredunes in Western France. *Remote Sensing* 10, 669. <https://doi.org/10.3390/rs10050669>

Lawrence, R.L., Wood, S.D., Sheley, R.L., 2006. Mapping invasive plants using hyperspectral imagery and Breiman Cutler classifications (randomForest). *Remote Sensing of Environment* 100, 356–362. <https://doi.org/10.1016/j.rse.2005.10.014>

Lefebvre, G., Davranche, A., Willm, L., Campagna, J., Redonnet, L., Merle, C., Guelmami, A., Poulin, B., 2019. Introducing WIW for Detecting the Presence of Water in Wetlands with Landsat and Sentinel Satellites. *Remote Sensing* 11, 2210. <https://doi.org/10.3390/rs11192210>

Liang, J., Liu, J., Xu, G., Chen, B., 2020. Grain size characteristics and net transport patterns of surficial sediments in the Zhejiang nearshore area, East China Sea. *Oceanologia* 62, 12–22. <https://doi.org/10.1016/j.oceano.2019.06.002>

Lunardon, N., Menardi, G., Torelli, F., 2014. ROSE: A Package for Binary Imbalanced Learning, in: *The R Journal*. <https://journal.r-project.org/archive/2014/RJ-2014-008/RJ-2014-008.pdf>

Lyons, J.E., Runge, M.C., Paskowski, H.P., Kendall, W.L., 2008. Monitoring in the Context of Structured Decision-Making and Adaptive Management. *The Journal of Wildlife Management* 72, 1683–1692. <https://doi.org/10.2193/2008-141>

Mathevet, R., Peluso, N.L., Couespel, A., Robbins, P., 2015. Using historical political ecology to understand the present: water, reeds, and biodiversity in the Camargue Biosphere Reserve, southern France. *Ecology and Society* 20. <https://www.jstor.org/stable/26270282>

Molinier, R., Tallon, G., 1965. La Camargue, pays de dunes. *Revue d'Écologie (La Terre et La Vie)* 19, 3–134. <https://doi.org/10.3406/revec.1965.4426>

- Mutanga, O., Adam, E., Cho, M.A., 2012. High density biomass estimation for wetland vegetation using WorldView-2 imagery and random forest regression algorithm. *International Journal of Applied Earth Observation and Geoinformation* 18, 399–406. <https://doi.org/10.1016/j.jag.2012.03.012>
- Newton, A., Icely, J., Cristina, S., Perillo, G.M.E., Turner, R.E., Ashan, D., Cragg, S., Luo, Y., Tu, C., Li, Y., Zhang, H., Ramesh, R., Forbes, D.L., Solidoro, C., Béjaoui, B., Gao, S., Pastres, R., Kelsey, H., Taillie, D., Nhan, N., Brito, A.C., de Lima, R., Kuenzer, C., 2020. Anthropogenic, Direct Pressures on Coastal Wetlands. *Frontiers in Ecology and Evolution* 8. <https://doi.org/10.3389/fevo.2020.00144>
- Olsson, P., Folke, C., Berkes, F., 2004. Adaptive Comanagement for Building Resilience in Social–Ecological Systems. *Environmental Management* 34, 75–90. <https://doi.org/10.1007/s00267-003-0101-7>
- Parc naturel régional de Camargue, Tour du Valat, Société nationale de protection de la nature, CPIE Rhône Pays d’Arles, 2022. Plan de gestion des Etangs et marais des salins de Camargue 2023 – 2032, état des lieux – diagnostic. Rapport pour le Conservatoire du littoral., Conservatoire du Littoral.
- Parsons, M.L., 1998. Salt Marsh Sedimentary Record of the Landfall of Hurricane Andrew on the Louisiana Coast: Diatoms and Other Paleoindicators. *Journal of Coastal Research* 14, 939–950.
- Poulin, B., Davranche, A., Lefebvre, G., 2010. Ecological assessment of *Phragmites australis* wetlands using multi-season SPOT-5 scenes. *Remote Sensing of Environment* 114, 1602–1609. <https://doi.org/10.1016/j.rse.2010.02.014>
- Pouzet, P., Maanan, M., 2020. Temporal approaches of historical extreme storm events based on sedimentological archives. *Journal of African Earth Sciences* 162, 103710. <https://doi.org/10.1016/j.jafrearsci.2019.103710>
- Rapinel, S., Mony, C., Lecoq, L., Clément, B., Thomas, A., Hubert-Moy, L., 2019. Evaluation of Sentinel-2 time-series for mapping floodplain grassland plant communities. *Remote Sensing of Environment* 223, 115–129. <https://doi.org/10.1016/j.rse.2019.01.018>
- Redondo-Gomez, S., Mateos-Naranjo, E., Davy, A.J., Fernandez-Munoz, F., Castellanos, E.M., Luque, T., Figueroa, M.E., 2007. Growth and Photosynthetic Responses to Salinity of the Salt-marsh Shrub *Atriplex portulacoides*. *Annals of Botany* 100, 555–563. <https://doi.org/10.1093/aob/mcm119>

- Rey, T., Lefevre, D., Vella, C., 2009. Deltaic plain development and environmental changes in the Petite Camargue, Rhone Delta, France, in the past 2000 years. *Quaternary Research* 71, 284–294. <https://doi.org/10.1016/j.yqres.2008.10.007>
- Rogel, J.A., Ariza, F.A., Silla, R.O., 2000. Soil salinity and moisture gradients and plant zonation in Mediterranean salt marshes of Southeast Spain. *Wetlands* 20, 357–372. [https://doi.org/10.1672/0277-5212\(2000\)020\[0357:SSAMGA\]2.0.CO;2](https://doi.org/10.1672/0277-5212(2000)020[0357:SSAMGA]2.0.CO;2)
- Sabatier, F., 2008. Modelling the impact of the climatic changes on the dune erosion. The case of the Camargue. *La Houille Blanche* 94, 40–49. <https://doi.org/10.1051/lhb:2008004>
- Silvestri, S., Marani, M., Marani, A., 2003. Hyperspectral remote sensing of salt marsh vegetation, morphology and soil topography. *Physics and Chemistry of the Earth, Parts A/B/C, Applications of Quantitative Remote Sensing to Hydrology* 28, 15–25. [https://doi.org/10.1016/S1474-7065\(03\)00004-4](https://doi.org/10.1016/S1474-7065(03)00004-4)
- Ullmann, A., Pirazzoli, P.A., Tomasin, A., 2007. Sea level changes in Camargue: Trends over the 20th century. *Continental Shelf Research* 27, 922–934. <https://doi.org/10.1016/j.csr.2006.12.001>
- van Proosdij, D., Davidson-Arnott, R.G.D., Olney, J., 2006. Controls on spatial patterns of sediment deposition across a macro-tidal salt marsh surface over single tidal cycles. *Estuarine, Coastal and Shelf Science* 69, 64–86. <https://doi.org/10.1016/j.ecss.2006.04.022>
- Vanden Borre, J., Paelinckx, D., Mueher, C.A., Kooistra, L., Haest, B., De Blust, G., Schmidt, A.M., 2011. Integrating remote sensing in Natura 2000 habitat monitoring: Prospects on the way forward. *Journal for Nature Conservation* 19, 116–125. <https://doi.org/10.1016/j.jnc.2010.07.003>
- Yu, R.-F., Chen, H.-W., Cheng, W.-P., Chu, M.-L., 2009. Simultaneously monitoring the particle size distribution, morphology and suspended solids concentration in wastewater applying digital image analysis (DIA). *Environmental Monitoring and Assessment* 148, 19–26. <https://doi.org/10.1007/s10661-007-0135-z>
- Zedler, J.B., Kercher, S., 2005. WETLAND RESOURCES: Status, Trends, Ecosystem Services, and Restorability. *Annual Review of Environment and Resources* 30, 39–74. <https://doi.org/10.1146/annurev.energy.30.050504.144248>

Zhong, L., Gong, P., Biging, G.S., 2014. Efficient corn and soybean mapping with temporal extendability: A multi-year experiment using Landsat imagery. *Remote Sensing of Environment* 140, 1–13.
<https://doi.org/10.1016/j.rse.2013.08.023>

Journal Pre-proof

Appendices

Appendix A: Land cover sampling and classification validation

Table A.1. Number of sampling points per land cover types

Categories	Number of points
Algae	55
<i>Amorpha</i>	15
Aquatic beds	18
<i>A. macrostachyum</i>	76
<i>Arundo donax</i>	27
Deep water	72
Dry bare soil	120
<i>Elymo arenarii-Agropyretum</i>	81
<i>Junceiformis</i>	
Graminea+ <i>A. macrostachyum</i>	56
Grey dune	48
<i>Imperata cylindrica</i>	44
<i>Juncus acutus</i>	26
<i>Juncus maritimus</i>	20
<i>Juncus</i> and reed pasture	54
<i>Ludwigia sp.</i>	50
Meadow	50
Moist bare soil	145
Mud	73
<i>Olea</i>	54
<i>Phillyrea</i>	30
Pine	64
<i>Populus</i>	42

Reed beds	51
Reedbeds in dune	10
Rice	59
Salt	52
Salt water	53
<i>S. fruticosa</i>	84
<i>Schoenus</i>	36
Annual <i>Salicornia</i> sparse	86
<i>Spartina</i>	24
<i>Sporoboletum arenarii</i>	31
Steppe	48
<i>Tamaris</i>	37
Turbid water	50
Annual <i>salicornia</i> very dense	136
White dune	34
Total number of sample points	2011

Table A.2. Error of omission on the validation sample from 2010 to 2013 data gathering

Categories	Number of points	<i>S. fruticosa</i> map	<i>A. macrostachyum</i> map	Error of omission in the final map
Sea	103	0	0	0,00
Algae	60	0	0	0,00
<i>A. macrostachyum</i>	162	0	118	0,27
Lower dune marsh	184	1	0	0,01
White dunes	109	0	0	0,00
Embryonic dunes	77	0	0	0,00
Grey dunes	161	0	0	0,00
<i>Phillyrea</i>	162	3	0	0,02

Aquatic beds	39	0	0	0,00
Other trees	59	0	0	0,00
Meadows	128	0	0	0,00
Phytoplankton	47	0	0	0,00
Pines	154	0	0	0,00
Salty meadows	191	4	3	0,04
Rice	49	0	0	0,00
Reedbeds	289	0	0	0,00
Annual <i>Salicornia</i>	166	0	4	0,02
<i>S. fruticosa</i>	131	73	3	0,44
Salt crust	34	0	0	0,00
Bare soil	221	0	0	0,00
Steppes	127	0	1	0,01
Total	2653			

Appendix B: Worldview data

Table B.1. Worldview 2 characteristics

World View 2		
	Multispectral	Panchromatic
Spatial resolution	2m	0.5m
No. Spectral bands	8	1
	400-450 nm (coastal)	450-800 nm
	450-510 nm (blue)	
	510-580 nm (green)	
	585-625 nm (yellow)	
	630-690 nm (red)	
	705-745 (red edge)	

	770–895 (near IR-1)
	860-900 nm (near IR-2)
Radiometric	11
Swath width	16.4
Temporal coverage	2009-
Solar angle	10.3
Acquisition date	31/08/2016

Table B.2. Multispectral indices used for modelling halophilous scrub distribution

Acronym	Name	Formula	Reference
BSI	Brightness Soil index	$3\sqrt{RT(R^2+PIR^2)}$	(Kauth and Thomas, 1976)
CI	Clearness Index	G^2/R	(Besnard et al., 2015)
DVI	Difference vegetation index	$PIR2-R$	(Richardson and Wiegand, 1977)
DWV	Difference Water Vegetation	$NDWI1-NDVI1$	(Gond, V. et al., 2004)
IFW	Index of Free Water	$PIR-G$	(Adell and Puech, 2003)
NDSI	Normalized difference soil index	$G-Y/G+Y$	(Wolf, 2010)
NDVI1	Normalized difference vegetation index	$R-PIR/PIR+R$	(Wolf, 2010)
NDVI2	Normalized difference vegetation index	$PIR1-RE/PIR1+RE$	(Mutanga et al., 2012)
NDVI3	Normalized difference vegetation index	$PIR2-R/PIR2+R$	(Rouse Jr et al., 1974)
NDWI1	Normalized difference water index	$C-PIR2/C+PIR2$	(Wolf, 2010)
NDWI2	Normalized difference water index	$V-PIR2/V+PIR2$	(McFeeters, 1996)
NHFD	Non-homogeneous features	$RE-C/RE+C$	(Wolf, 2010)

difference

OSAVI	Optimized Soil Adjusted Vegetation Index	$(PIR2 - R) / (PIR2 + R + 0.16)$	(Rondeaux et al., 1996)
PSSR	Pigment specific Simple ratio	$PIR1 - C / PIR1 + C$	(Blackburn, 1998)
SAVI	Soil adjusted vegetation index	$(1.5 * (PIR2 - R)) / (PIR2 + R + 0.5)$	(Huete, 1988)
SIPI	Structure Insensitive Pigment Index	$PIR1 - C / PIR1 + R$	(Penuelas et al, 1995)
VI	Vegetation index	$PIR2 / R$	(Lillesand et al., 2014)
SR	Simple Ratio	$R / PIR2$	(Pearson and Miller, 1972)
Wi	Water Index	$PIR2 / C$	(Davranche et al., 2013)
WII	Water impoundment Index	$PIR1^2 / R$	(Caillaud et al., 1987)

Appendix C Sediment size variables

Table C.1. Sediment size variables

Parameters	Description
MEAN	Mean size of the sediment sampled
SORTING	Distribution index of the sediment sampled attesting its homogeneity
SKEWNESS	Degree of symmetry of the sediment sampled
KURTOSIS	Flatter degree of the grain size distribution
MODE1mm	First grain size statistical mode
MODE2mm	Second grain size statistical mode
MODE3mm	Third grain size statistical mode
D10mm	First decile, value where 10% of the grain size distribution is lower, and 90% higher
D50mm	Median grain size
D90mm	9 th decile, value where 90% of the grain size distribution is lower, and 10% higher
D90/D10mm	D90 over D10 ratio
D90-D10mm	D90 on D10 difference

D75/D25mm	Third quartile over First quartile ratio
D75- D25mm	Third quartile over first quartile difference
VCOARSE GRAVEL	Percentage of very coarse gravel (> 32mm)
COARSEGRAVEL MEDIUM GRAVEL	Percentage of coarse gravel (16 – 32mm)
FINEGRAVEL	Percentage of medium gravel (8 – 16mm)
VFINEGRAVEL	Percentage of fine gravel (4 – 8mm)
VCOARSE SAND	Percentage of very fine gravel (2 – 4mm)
COARSE SAND	Percentage of very coarse sand (1 – 2mm)
MEDIUM SAND	Percentage of coarse sand (500 μ m - 1mm)
FINE SAND	Percentage of medium sand (250 - 500 μ m)
VFINE SAND	Percentage of fine sand (125 - 250 μ m)
VCOARSE SILT	Percentage of very fine sand (63 – 125 μ m)
COARSE SILT	Percentage of very coarse silt (31 - 63 μ m)
MEDIUM SILT	Percentage of coarse silt (16 - 31 μ m)
FINE SILT	Percentage of medium silt (8 - 16 μ m)
VFINE SILT	Percentage of fine silt (4 - 8 μ m)
CLAY	Percentage of very fine silt (2 - 4 μ m)
SILT	Total percentage of clay (< 2 μ m)
GRAVEL	Total percentage of silt (2 - 63 μ m)
SAND	Total percentage of gravel (< 2mm)
MUD	Total percentage of sand (63 μ m - 2mm)
	Total percentage of mud (< 63 μ m)

Author contributions:

Aurélie Davranche: Conceptualization, Methodology, Software, Formal analysis, Investigation, Resources, Data curation, Writing - Original Draft, Writing - Review & Editing, Visualization, Supervision **Céline Arzel:** Conceptualization, Formal analysis, Writing - Original Draft, Writing - Review & Editing, **Pierre Pouzet:** Formal analysis, Investigation, Resources, Writing - Review & Editing, **A. Rita Carrasco:** Conceptualization, Writing - Original Draft, Writing - Review & Editing, Visualization, **Gaëtan Lefebvre:** Conceptualization, Methodology, Investigation, Resources, Supervision, **Dimitri Lague:** Methodology, Software, Formal analysis, Data Curation, Writing - Review & Editing, **Marc Thibault:** Resources, Writing - Review & Editing, **Alice Newton:** Writing - Original Draft, Writing - Review & Editing, **Cyril Fleurant:** Investigation, Resources, Supervision, Writing - Review & Editing, **Mohamed Maanan:** Conceptualization, Methodology, Resources, Funding acquisition, Writing - Review & Editing, **Brigitte Poulin:** Methodology, Investigation, Resources, Supervision, Writing - Review & Editing, Project administration, Funding acquisition.

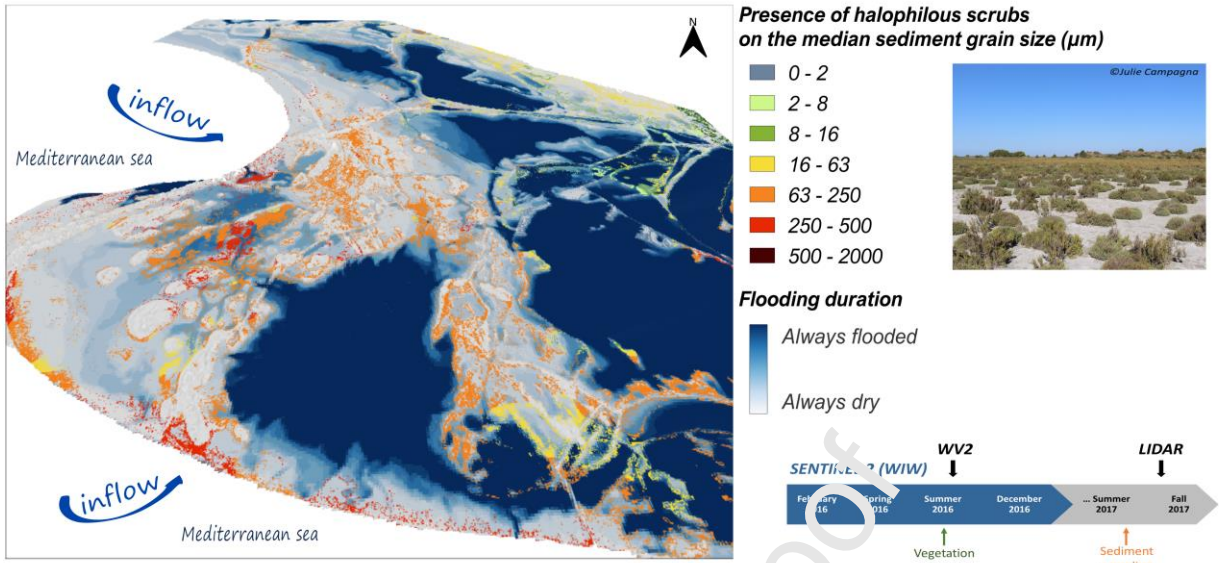
Declaration of interests

The authors declare that they have no known competing financial interests or personal relationships that could have appeared to influence the work reported in this paper.

The authors declare the following financial interests/personal relationships which may be considered as potential competing interests:

Journal Pre-proof

Graphical abstract



Journal Pre-proof

Highlights:

- Species must be classified individually to better map the halophilous scrub habitat
- Satellite-derivate species presence was predicted accounting sediment distribution
- Sediment grain sizes predicted flooding duration derived from SENTINEL 2 data
- Flooding duration and species distribution could not be predicted by LIDAR elevations
- A multisensory approach can assess edaphic changes in coastal sites to assist adaptive management

Journal Pre-proof